Molecular Biology of the Cell
Vol. 19, 4341–4351, October 2008

Exon Loss Accounts for Differential Sorting of Na-K-Cl Cotransporters in Polarized Epithelial Cells

Monica Carmosino,* Ignacio Giménez,*† Michael Caplan,*‡ and Biff Forbush*‡

*Department of Cellular and Molecular Physiology, Yale University School of Medicine, New Haven, CT 06520

Submitted May 14, 2008; Revised July 16, 2008; Accepted July 17, 2008
Monitoring Editor: Keith E. Mostov

The renal Na-K-Cl cotransporter (NKCC2) is selectively expressed in the apical membranes of cells of the mammalian kidney, where it is the target of the clinically important loop diuretics. In contrast, the "secretory" NKCC1 cotransporter is localized in the basolateral membranes of many epithelia. To identify the sorting signal(s) that direct trafficking of NKCCs, we generated chimeras between the two isoforms and expressed these constructs in polarized renal epithelial cell lines. This analysis revealed an amino acid stretch in NKCC2 containing apical sorting information. The NKCC1 C terminus contains a dileucine motif that constitutes the smallest essential component of its basolateral sorting signal. NKCC1 lacking this motif behaves as an apical protein. Examination of the NKCC gene structure reveals that this dileucine motif is encoded by an additional exon in NKCC1 absent in NKCC2. Phylogenetic analysis of this exon suggests that the evolutionary loss of this exon from the gene encoding the basolateral NKCC1 constitutes a novel mechanism that accounts for the apical sorting of the protein encoded by the NKCC2 gene.

INTRODUCTION

The two isoforms of the Na-K-Cl cotransporter (NKCC) protein are ~60% identical to one another (Delpire *et al*., 1994; Payne and Forbush, 1994), but they are targeted to different membrane domains, where they play different physiological roles. The "absorptive" isoform NKCC2 localizes to the apical membranes of the thick ascending limb cells in the mammalian kidney, including the region of the macula densa (Igarashi *et al*., 1995; Obermuller *et al*., 1996), in which it is responsible for sodium and chloride reabsorption and the maintenance of normal blood pressure. Improper function of NKCC2 results in human disease, including Bartter syndrome type I and hypertension (Simon *et al*., 1996; Glorioso *et al*., 2001; Ji *et al*., 2008). Vasopressin is the most important stimulus of NaCl transport by NKCC2, increasing the transport activity and bringing about trafficking from an intracellular compartment to the apical membrane (Gimenez and Forbush, 2003; Ortiz, 2006).

The "secretory" isoform NKCC1 localizes at highest concentrations in the basolateral membranes of secretory epithelia in which it is responsible for the transepithelial secretion of Cl^- and water upon stimulation by secretagogues (Haas and Forbush, 2000). NKCC1 is also present in many types of nonepithelial cells where it contributes to the regulation of cell volume and intracellular Cl^- concentration (for reviews, see Delpire, 2000; Haas and Forbush, 2000).

Polarized trafficking is determined by signals contained within a membrane protein's structure, and several distinct classes of sorting motifs have been identified. The routing of basolaterally targeted proteins is often mediated by discrete cytosolic amino acid sequences containing a critical tyrosine residue within a NP*X*Y or Y*XX* motif, a dileucine motif, a dihydrophobic motif, a cluster of acidic residues, or a combination of these elements. In contrast, the apical targeting of transmembrane proteins can be mediated by a variety of signals. For example, both *N*- and *O*-linked glycans are postulated to mediate apical targeting for several proteins, and apical targeting may also occur via the incorporation of apically directed proteins into lipid rafts (for review, see Muth and Caplan, 2003; Rodriguez-Boulan *et al*., 2005). There are examples, however, of proteins whose apical targeting may be independent of both glycosylation and raft association. In these cases, apical sorting signals seem to be embedded in amino acid sequences located within transmembrane or intracellular domains that can act either as discrete or conformational sorting motifs recognized by the apical sorting machinery (Chuang and Sung, 1998; Dunbar *et al*., 2000; Karim-Jimenez *et al*., 2001; Inukai *et al*., 2004). It has been demonstrated previously that glycosylation of the NKCC cotransporters is not required for their polarized targeting to the plasma membrane but that it is a prerequisite for export of these proteins from the Golgi apparatus (Paredes *et al*., 2006).

To identify the sorting signals in NKCC1 and NKCC2, we have generated chimeras between the two isoforms and analyzed their localization in Madin-Darby canine kidney (MDCK) cells. Our data show that a 77-amino acid region in the NKCC1 and NKCC2 C termini contains basolateral and apical sorting information, respectively. Altering a dilucine

This article was published online ahead of print in *MBC in Press* (http://www.molbiolcell.org/cgi/doi/10.1091/mbc.E08–05–0478) on July 30, 2008.

‡ These authors contributed equally to this work.

† Present address: Instituto Aragones de Ciencias de la Salud, 50009 Zaragoza, Spain.

Address correspondence to: Monica Carmosino (monica.carmosino@yale.edu).

Abbreviations used: HA, hemagglutinin; HEK, human embryonic kidney; MDCK, Madin-Darby canine kidney; NKCC, Na-K-Cl cotransporter; PLAP, placental alkaline phosphatase; TM, transmembrane domain; VSVG, vesicular stomatitis virus glycoprotein.

motif within this region results in apical localization of the mutant protein, thus defining the smallest essential component of the NKCC1 basolateral sorting signal. This motif is part of a 16-amino acid exon that has been evolutionarily lost from NKCC2 and retained in NKCC1, suggesting a novel mechanism through which genes encoding differentially targeted isoforms of homologous proteins can arise.

MATERIALS AND METHODS

Constructs

Chimeras between human NKCC1 and rabbit NKCC2a were produced using the QuikChangeXL site-directed mutagenesis kit (Stratagene, La Jolla, CA) to create common NKCC1/NKCC2 restriction sites followed by exchange of fragments generated by polymerase chain reaction (PCR) or restriction digest. All constructs were hemagglutinin (HA)-tagged at their N terminus (see Supplemental Material for all sequence details); DNA and amino acid residue positions are reported here relative to the first amino acid residue in the native sequences. PCR-generated regions and junction points were sequenced in full. Constructs were subcloned into pIRES (Invitrogen, Carlsbad, CA) and/or pJB20 (Isenring *et al*., 1998b) expression vectors. Experiments in Figure 1 present transient expression using pIRES; otherwise results are from stable expression using pJB20. In agreement with previous work (Isenring *et al*., 1998b), we found that the presence of the N terminus of NKCC2 in any construct seems to prevent good functional expression in human embryonic kidney (HEK)-293 cells as well as stable expression in MDCK cells.

Chimeras are named using two conventions: N-terminus–transmembrane domain (TM)–C-terminus chimeras (Figure 1) are called simply by their corresponding isoform numbers (e.g., 1-2-1 has the TM of NKCC2 and termini of NKCC1), whereas chimeras within the C terminus are described by numerals denoting their junction points. Chimera 1-2-1 and 1-2-2 use a new BstZ17I restriction site in NKCC2a at base pairs 498, corresponding to a site in NKCC1 at base pairs 822; similarly 1-2-1 and 2-2-1 use a new PmlI site (later termed position "I") in NKCC2 at base pairs 2026 corresponding to a site in NKCC1 at base pairs 2350. Chimera 1-1-2 is also termed "chimera I" as the first of the chimeras in the C terminus. To make other C-terminal chimeras, we constructed a human (h)NKCC1 cDNA with new silent SanDI, AvrII, and SbfI restriction sites at positions II, III, and IV (base pairs 2475, 2625, and 2790), with existing PmlI, HindIII, and BspEI sites I, V, and VI (base pairs 2350, 3020, and 3236; we removed a HindIII site in pJB), and a unique BsiWI site in the C-terminal cloning region. PCR-amplified fragments of the NKCC2a C terminus with appropriate restriction sites in the primer regions were then ligated into corresponding NKCC1 sites to generate chimeras.

Within the IV-V region of the NKCC1 C terminus, we constructed two deletion mutants, each replacing half of the region with a short linker by means of two pairs of oligonucleotides and triple ligation into the SbfI and HindIII sites (in NKCC1ΔA, residues 938–968 are replaced with PRSRGL; in NKCC1ΔB, residues 969-1006 are replaced by PRSQS). Point mutants in this region ($L_{989}A/L_{990}A$, $L_{1008}A/L_{1009}A$, $E_{978}Q/E_{979}Q/E_{980}Q/D_{981}N$, $T_{986}A/Q_{987}A/P_{988}A$, $P_{997}A$) were generated by QuikChange mutagenesis.

Placental alkaline phosphatase (PLAP)-V-NKCC constructs were prepared to investigate the intrinsic sorting potential of the NKCC IV-V region. PLAP-V, containing the coding region of PLAP followed by the transmembrane domain of vesicular stomatitis virus glycoprotein (VSVG) (Brown *et al*., 2004), was subcloned into the EcoRI site of pcDNA3.1. The IV-V region of appropriate NKCC constructs was then amplified by PCR and cloned into HindIII and KpnI sites downstream of the VSVG sequence.

Cells and Transfection

MDCK cells and HEK-293 cells were maintained in DMEM, 10% fetal bovine serum, penicillin (50 U/ml) and streptomycin (50 U/ml), at 37°C, 5% CO_2 in a humidified incubator, and transfection was performed with Lipofectamine 2000 (Invitrogen) according to the manufacturer's instructions. Stable clones were selected in 1 mg/ml geneticin, and they were studied as either mixed stable lines (Figures 4, 5, 7, and 8) or as individually selected clonal lines (Figures 2, 3, and 6).

Cell Surface Biotinylation and Western Blotting

MDCK cells stably expressing the different chimeras were grown to confluence on 45-mm polycarbonate filter insets for 3–5 d. For each cell line two filters were plated. Cell surface biotinylation was performed as described previously (Roush *et al*., 1998). NKCC chimeras were detected by Western blotting using the monoclonal anti HA antibody (dilution 1:1000; Covance Research Products, Princeton, NJ) and a horseradish peroxidase-conjugated goat anti-mouse secondary antibody (1:5000).

Immunofluorescence

Transfected MDCK cells were grown on 24-mm polycarbonate transwell filter inserts for 3 d. Cells were fixed with 4% paraformaldehyde in phosphate-buffered saline (PBS) (20 min; room temperature), permeabilized with 0.1% Triton X-100 in PBS (15 min), and incubated in 1% bovine serum albumin (BSA) in PBS (30 min), followed by a monoclonal anti-HA antibody (1:500 in BSA/PBS; 2 h; Covance Research Products), washed with PBS, and incubated in anti-mouse fluorescein isothiocyanate (FITC)-conjugated antibody (1:500 in BSA/PBS; 1 h; Sigma-Aldrich, St. Louis, MO). Washed filters were mounted on glass slides using Vectashield (Vector Laboratories, Burlingame, CA), and they were sealed with coverslips and nail polish. Confocal images were obtained with a laser scanning fluorescence microscope (LSM410; Carl Zeiss, Thornwood, NY). Images are the product of eightfold line averaging, and the xz sections were produced using a 0.2-μm motor step. Contrast and brightness settings were chosen so that all pixels were in the linear range. PLAP-V constructs were localized on the surface of nonpermeabilized MDCK cells by using a monoclonal anti-PLAP antibody (1:200 in BSA/PBS for 3 h at 4°C; Santa Cruz Biotechnology, Santa Cruz, CA), followed by fixation and incubation with secondary antibody as described above.

$^{86}Rb^+$ Influx Assay

NKCC transport function was examined by $^{86}Rb^+$ influx in stably transfected HEK-293 cells as described previously (Pedersen *et al*., 2008). Briefly, cells were preincubated in various external [Cl^-] (with gluconate replacement) for 1 h to activate the cotransporter. Furosemide was used in some preincubation conditions to block transporter-mediated Cl^- movements; furosemide quickly dissociates before the flux assay. Fluxes were carried out for 1 or 2 min at room temperature in regular flux medium, which contains 135 mM NaCl, 5 Mm RbCl (2 μCi/ml ^{86}Rb), 1 mM $CaCl_2$, 1 mM $MgCl_2$, 1 mM Na_2PO_4, 1 mM Na_2SO_4, and 15 mM Na-HEPES, pH 7.4. $^{86}Rb^+$ uptake was terminated with a rinse in high K^+ buffer (135 mM K gluconate, 5 mM Na-gluconate, 1 mM $CaCl_2/MgCl_2$, 1 mM Na_2HPO_4/Na_2SO_4, 15 mM Na-HEPES, pH 7.4) and cells were then allowed to dry. The flux experiments reported here were performed by an automated 96-well plate flux machine that performs each solution change as a wash procedure without removing all of the fluid from the well. Cellular $^{86}Rb^+$ uptake was determined by phosphorimage analysis of the 96-well plate.

Detergent Solubility Assay

MDCK cells expressing the chimeras III and V were grown to confluence in 10-cm^2 tissue culture dishes and lysed in 1 ml of buffer (25 mM Tris-HCl, pH 7.4, 150 mM NaCl, and 5 mM EDTA) containing 1% Triton X-100 on ice for 30 min. Lysates were passed trough a 21-gauge needle to shear DNA, mixed with 1 ml of 80% sucrose, transferred into polycarbonate tubes, and overlaid with 2 ml of 30% sucrose and 1 ml of 5% sucrose. The floatation gradients were spun at 120,000 $\times$ *g* for 18 h at 4°C. Eight fractions were then collected from the top and incubated with 50 μl of StrataClean beads (Invitrogen) for 20 min at room temperature into the rocking platform. The samples were centrifuged for 5 min at 16,000 $\times$ *g*, and the supernatant was removed. Proteins were released from the beads by boiling for 10 min in 50 μl of 2$\times$ Laemmli buffer containing 1 M dithiothreitol. All fractions were assessed by Western blotting for the presence of either the chimeras or the lipid raft marker flotillin-1 by using the monoclonal HA-tag antibody and the monoclonal anti flotillin-1 antibody (BD Biosciences, San Jose, CA) respectively.

RESULTS

The Cytoplasmic C Terminus of both NKCC1 and NKCC2 Contains Information Necessary for Sorting

NKCC1 and NKCC2 are expressed on basolateral and apical membranes, respectively, in their native epithelial tissues. In addition, exogenously expressed NKCC1 has been found to be sorted to the basolateral membrane (Brindikova *et al*., 2003; Del Castillo *et al*., 2005). The results in Figure 1 demonstrate that in transiently transfected MDCK cells, HA-tagged NKCC1 and NKCC2 are delivered to basolateral and apical membranes, respectively, as illustrated by confocal immunofluorescence microscopy viewed en face and in xz cross section. Clearly the presence of the N-terminal HA-tag does not interfere with the proper sorting and localization of either of the NKCC proteins, consistent with the fact that the extreme N termini are very poorly conserved in length and sequence; thus, it seems unlikely to contain significant trafficking information. These results also illustrate that MDCK cells are able to appropriately sort NKCCs.

Sequence analysis of NKCC1 and NKCC2 demonstrates that they have the same basic domain structure, and that although they are only 55% identical overall, most of the dissimilarity is concentrated in three regions (Payne and

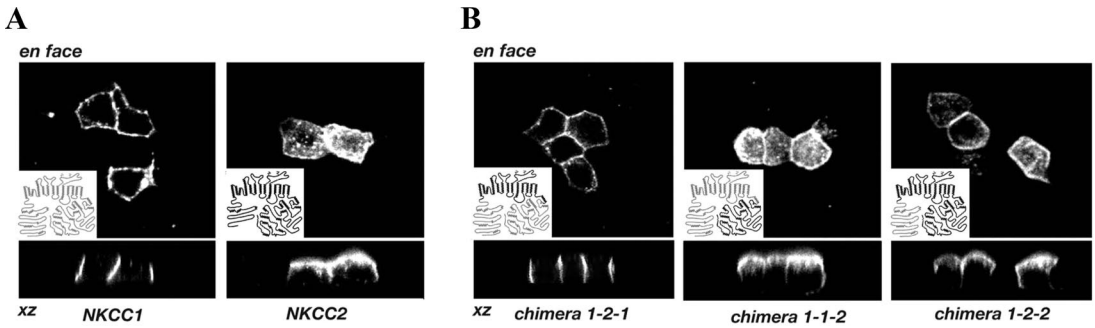

Figure 1. Localization of NKCC1, NKCC2 and chimeras in transiently transfected MDCK cells. The chimeras were generated by exchanging the three major portions of the contransporter: the N terminus, TM, and the C terminus. The structure of each chimera is shown in the inset of the en face image in which its localization is depicted. The NKCC1 regions are shown in gray, and the NKCC2 regions are shown in black. The sorting information is contained within the C termini of NKCC proteins.

Forbush, 1994 and Supplemental Figure 1), including an extracellular loop, most of the N terminus, and a region in the C terminus on which we focus below. The similarity of the NKCCs makes it possible to generate functional chimeras between the two transporters without introducing major structural changes. As we did previously for shark and human NKCC1s (Isenring *et al*., 1998a), we initially generated chimeras with junction points between the TM and the two termini, and expressed these constructs in MDCK cells.

The results with the first set of chimeras are illustrated in Figure 1B. Although replacement of the NKCC1 transmembrane domain with NKCC2 residues did not alter the basolateral localization of NKCC1 (chimera 1-2-1), replacement of the NKCC1 C terminus with that of NKCC2 produced a chimeric protein that was sorted primarily to the apical membrane (chimera 1-1-2). In contrast, results with chimera 1-2-2 demonstrate that replacement of the N terminus of NKCC2 with that of NKCC1 does not affect the distribution of NKCC2, in that this NKCC construct is sorted predominately to the apical membrane. Because the presence of the NKCC1 N terminus does not affect the apical localization of NKCC2 and the presence of the NKCC2 C terminus induces the apical localization of NKCC1, we conclude that sorting information is contained within the C-terminal domains of the NKCC proteins.

Identification of a 77-Amino Acid Region in the Middle of the NKCC C Terminus That Contains Sorting Determinants

To define specific sorting regions within the ~460 amino acid NKCC C termini, we studied a sequential set of chimeras in which parts of the cytoplasmic C terminus of NKCC1 were replaced by the corresponding regions of NKCC2. We carried out this investigation by using an NKCC1 backbone because the NKCC2 N terminus has proven to be problematic in epithelial cell expression systems (see *Materials and Methods*). Beginning with the chimeric junction "I" at residue 782, the junction point is moved 40–80 amino acids toward the extreme C terminus in successive constructs I to VI (see Figure 2 labels for human NKCC1 residue numbers). Stable MDCK cell lines were generated with each chimera, grown to confluence on permeable filters, and then examined by immunofluorescence. As illustrated in Figure 2, the first four of the chimeras (I–IV) contain functional NKCC2 sorting information, because these proteins are clearly targeted to the apical membrane. In contrast, chimeras V and VI are delivered to the basolateral membrane, as is NKCC1 itself (Figure 2, bottom). These results demonstrate that the critical

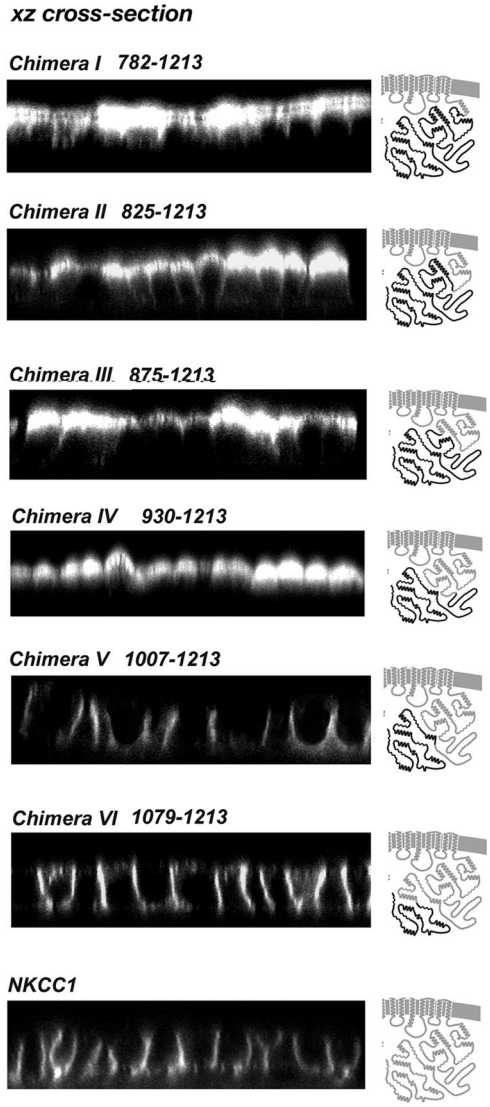

Figure 2. Localizations of sequential C terminus chimeras. Confocal xz cross-section immunofluorescence images are presented. Immunofluorescence analysis was performed on stably transfected MDCK cells. The junction point of each chimera is shown on the left of the panel in which its localization is depicted (numbering in replaced human NKCC1, NKCC1 C terminus in gray, NKCC2 C terminus in black). The sorting information is embedded in the amino acid region between the junction points of chimeras IV and V.

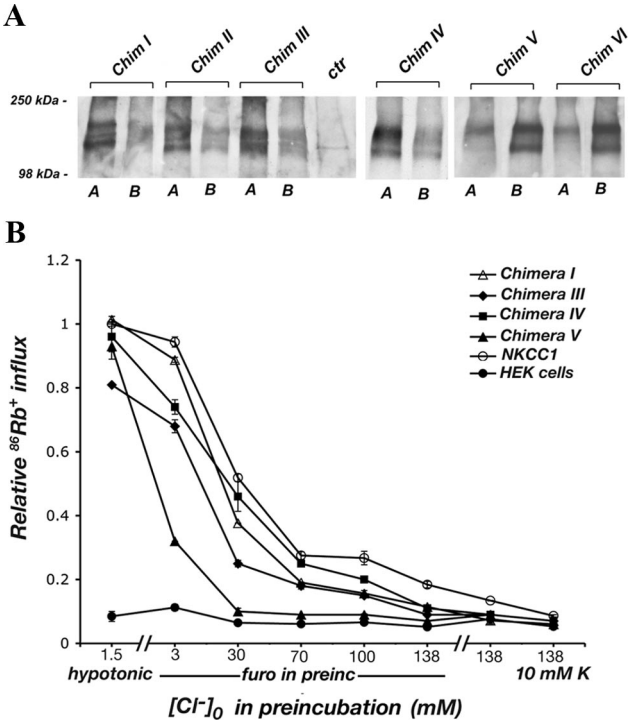

Figure 3. (A) Cell surface distribution of the sequential chimeras determined by domain-selective biotinylation in stably transfected MDCK cells. (B) Rate of $^{86}Rb^+$ influx mediated by chimeras I, III, IV, V, and NKCC1 in stably transfected HEK cells after preincubation in various media. The data are relative to the maximal activation of NKCC1 and are corrected for NKCC protein expression. Data are presented as the range of two measurements in a representative experiment. All chimeras are functionally active.

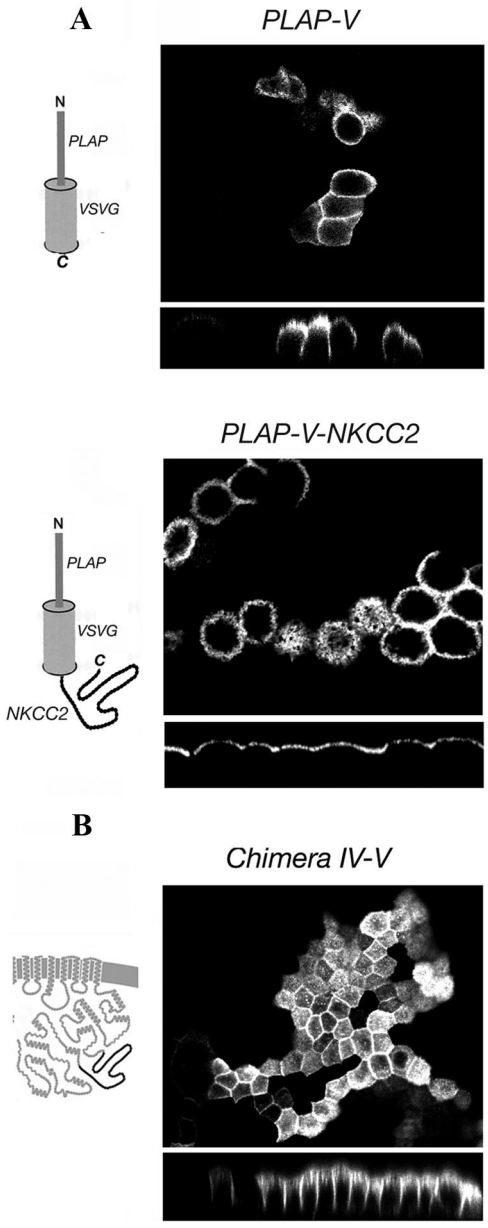

Figure 4. Localization of PLAP-V constructs and chimera IV-V. (A) The structure of each PLAP-V construct is shown on the left of the panel in which its localization is depicted. The IV-V region of NKCC2 carries autonomous apical sorting information. (B) The structure of the chimera IV-V is shown on the left of the panel in which its localization is depicted. The NKCC1 portions are shown in gray and the NKCC2 portions in black. The IV-V NKCC2 region is not, in itself, sufficient to induce the fully apical localization of NKCC1.

sorting information is embedded in the amino acid region between junction points IV and V (region IV-V), that is between residues 930 and 1007 of the human NKCC1 sequence. It is interesting to note that within this region there is very little sequence conservation between NKCC1 and NKCC2 and that the region has a relatively high index of predicted structural disorder (Supplemental Figures 1 and 2).

To assess biochemically the polarized distribution of the chimeras, we used domain-selective cell surface biotinylation to differentially label apical and basolateral membrane proteins. As illustrated by the results in Figure 3A, chimeras I–IV were found predominantly in the protein fraction accessed by biotinylation from the apical surface, whereas V and VI were detected among basolaterally biotinylated plasma membrane proteins. Thus, steady-state biotinylation experiments directly support the localization reported by immunofluorescence, and they demonstrate further that at least a substantial fraction of the chimeric proteins reside in the plasma membrane rather than in a subsurface vesicular compartment.

To examine the physiological activity of our chimeric NKCCs, we measured transporter-mediated $^{86}Rb^+$ influx in stably transfected HEK cells (see *Materials and Methods*). This system has been well-characterized, and, compared with epithelial cells, it has much lower background from endogenous cotransporters. NKCCs are strongly activated by decreases in cell chloride, and they mediate coupled Na^+, K^+ (or $^{86}Rb^+$), and Cl^- uptake into the cell. Figure 3B illustrates the steady-state activation curve of ion transport in response to changes in intracellular [Cl^-], brought about by preincubation in various media for 1 h before the 2 min flux measurement. The data demonstrate that all the chimeras tested are functionally active when maximally stimulated but that their activation curves are in some cases different from that of the NKCC1 parental protein. This suggests that conformational interactions within the C terminus may be important in NKCC regulation, and that these interactions are altered in the NKCC1-NKCC2 chimeras. This hypothesis is supported by our recent fluorescence resonance energy

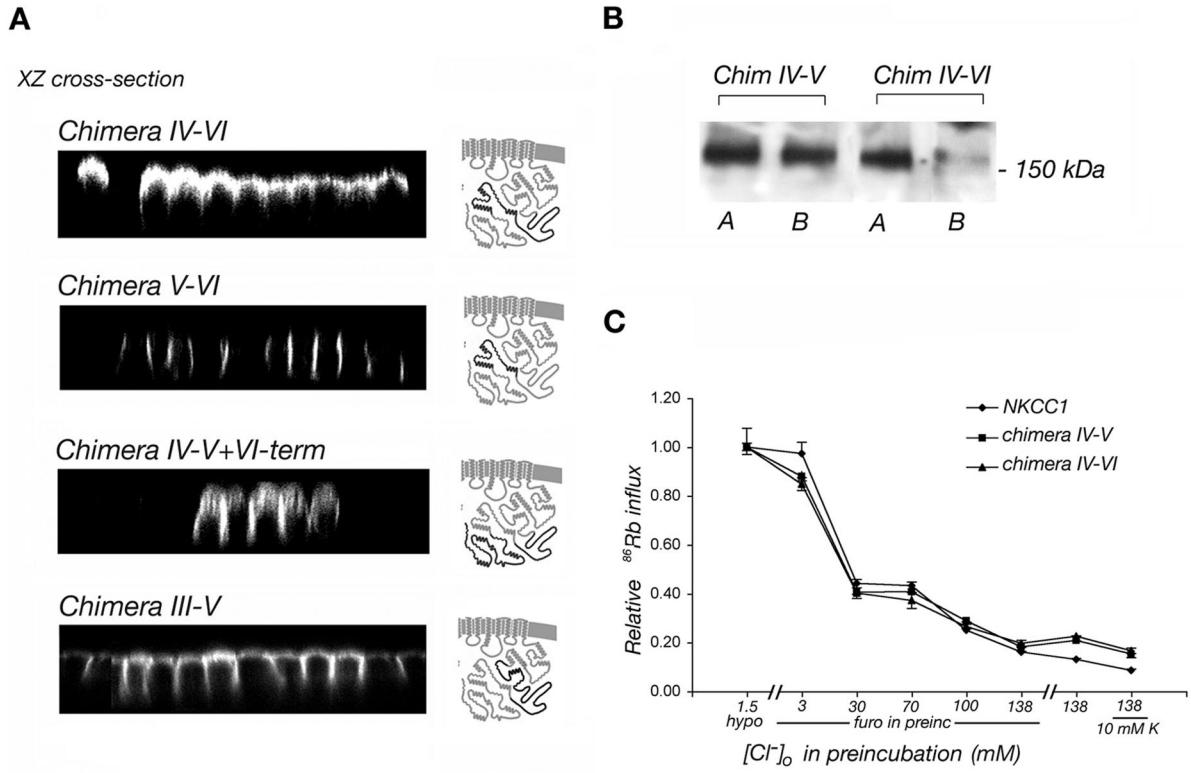

Figure 5. (A) Immunolocalization of chimeras IV-VI, V-VI, IV-V+V-term, III-V in stably transfected MDCK cells. xz cross-section immunofluorescence images are presented. The structure of each chimera is shown on the right of the panel in which its localization is depicted. The NKCC1 portions are shown in gray and the NKCC2 portions in black. The NKCC2 sequence downstream of the IV-V NKCC2 region is necessary for apical sorting. (B) Domain selective cell surface biotinylation of chimeras IV-V and chimera IV-VI (A, apical; B, basolateral). (C) Rate of $^{86}Rb^{+}$ influx mediated by chimeras IV-V, IV-VI, and NKCC1 in stably transfected HEK cells. The data are relative to the maximal activation of NKCC1 and are shown as average of three flux rows of a representative experiment. Chimeras IV-V and IV-VI are functionally identical to wild-type NKCC1.

transfer-based measurements of regulatory conformational change in NKCC1 (Monette, Carmosino, and Forbush, unpublished).

The Presence of a 150-Amino Acid Segment of the NKCC2 C Terminus Is Necessary to Fully Specify Apical Localization

To evaluate the intrinsic sorting potential of the IV-V region of NKCC2, we asked whether this region is sufficient to induce the apical localization of the unrelated PLAP VSVG protein (PLAP-V). The PLAP-V construct is composed of the PLAP extracellular domain fused to the transmembrane domain of VSVG. To visualize the plasma membrane distribution of the PLAP-V constructs, we used immunostaining in living stably transfected MDCK cells grown on permeable filters, taking advantage of a monoclonal antibody against an extracellular epitope of PLAP. By itself, PLAP-V exhibits a random distribution in MDCK cell plasma membranes (Brown *et al*., 2004), as illustrated by both apical and lateral staining in Figure 4A, top. In contrast, the tandem PLAP-V-NKCC2 construct was clearly restricted in its distribution to the apical membrane (Figure 1A, bottom), demonstrating that indeed the IV-V region of NKCC2 carries autonomous apical sorting information.

We asked whether the NKCC2 IV-V region would confer apical sorting when expressed in the context of the NKCC1 molecule. Surprisingly, as shown in Figure 4B, the distribution of NKCC chimera IV-V is both apical and lateral. Thus, although this replacement disrupts the purely basolateral distribution of NKCC1, this stretch of NKCC2 sequence is not, in itself, sufficient to induce full apical localization of NKCC1. Presumably, the sorting signal in the NKCC2 IV-V region that is effective in targeting PLAP-V to the apical membrane is partially masked when presented in the conformation of an intact NKCC chimera.

The results obtained with the NKCC2 IV-V chimera strongly suggest that residues distal to position V in NKCC2 must be important in apical sorting, because chimera IV (Figure 3) is almost fully apical, whereas chimera IV-V (Figure 4B) is not. To investigate this hypothesis, we studied a new set of chimeras, with results shown in Figure 5A. We found that when the NKCC2 IV-V region was augmented with the V-VI region, the apical localization of the resulting NKCC (chimera IV-VI) was substantially enhanced compared with that in chimera IV-V. By itself however, the V-VI region of NKCC2 had no effect on the basolateral sorting of NKCC1, as illustrated in the second panel in Figure 5A. Together, these results suggest that although the 72-amino acids of NKCC2 downstream of the IV-V region do not themselves contain a strong apical sorting signal, they are necessary to ensure full expression of the sorting potential of the NKCC2 IV-V signal and thus that the apical polarity of NKCC2 is dependent upon the presence of the entire IV-VI region. We also attempted to test whether the V-VI region of NKCC2 contains an autonomous apical sorting signal by appending it to PLAP-V. The resulting construct is unable to

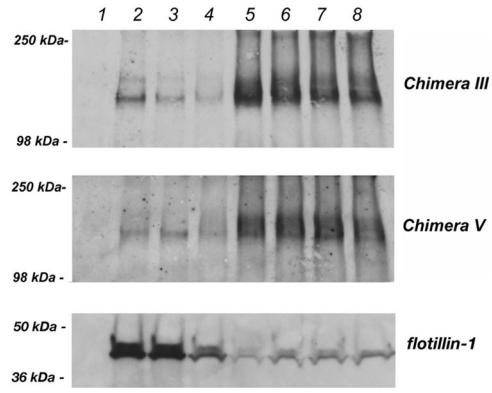

Figure 6. Detergent solubility assay of the apical chimera III and the basolateral chimera V. MDCK cells stably expressing chimera III and chimera V were subjected to the detergent solubility assay as described in Materials and Methods. A representative experiment is shown. Neither chimera is associated with detergent-insoluble membrane domains.

reach the cell surface and is trapped in an unidentified intracellular compartment (data not shown).

As a test of the specificity of the V-VI region in assisting apical sorting signaled by the NKCC2 IV-V domain, we examined two other chimeras in which either the upstream III-IV region or the terminal VI-term region were incorporated from NKCC2, along with IV-V (chimera III-V and chimera IV-V+VI-term). As illustrated in the bottom two panels of Figure 5A, each of these chimeras behaved like chimera IV-V, that is, they were distributed on both apical and lateral membrane domains. These results confirm the specificity of the V-VI region in assisting apical sorting, and they argue that there is no significant apical sorting information in the C terminus outside of the 150-amino acid residues in IV-VI.

Domain-selective surface biotinylation experiments were again used as a second measure of membrane distribution. The results shown in Figure 5B are in complete agreement with the above-mentioned immunofluorescence analysis in demonstrating that chimera IV-V is distributed in both apical and basolateral membranes, whereas chimera IV-VI is predominantly labeled from the apical surface. These data again show that the 150-amino acid IV-VI segment is both necessary and sufficient to bring about apical sorting. Chimeras IV-V and IV-VI are functionally identical to wild-type NKCC1 when stably expressed in HEK cells and assayed by $^{86}Rb^{+}$ flux (Figure 5C), which demonstrates that these constructs are correctly folded.

The Apical Localization of NKCC Chimeras Is Not Due to Detergent Resistant Membrane Association

To determine whether the apically delivered chimeras achieve their localization in MDCK cells through association with detergent-resistant membranes, confluent MDCK cells stably expressing the apical chimera III or basolateral chimera V were extracted with the nonionic detergent Triton X-100 on ice followed by density gradient centrifugation using a multistep gradient (see *Materials and Methods*). As shown in Figure 6, neither chimera is found in appreciable amounts in the detergent-resistant flotillin-enriched buoyant fractions. Rather, they are detected in highest concentration in the high-density detergent-soluble fraction, indicating that apical delivery is accomplished without lipid raft association.

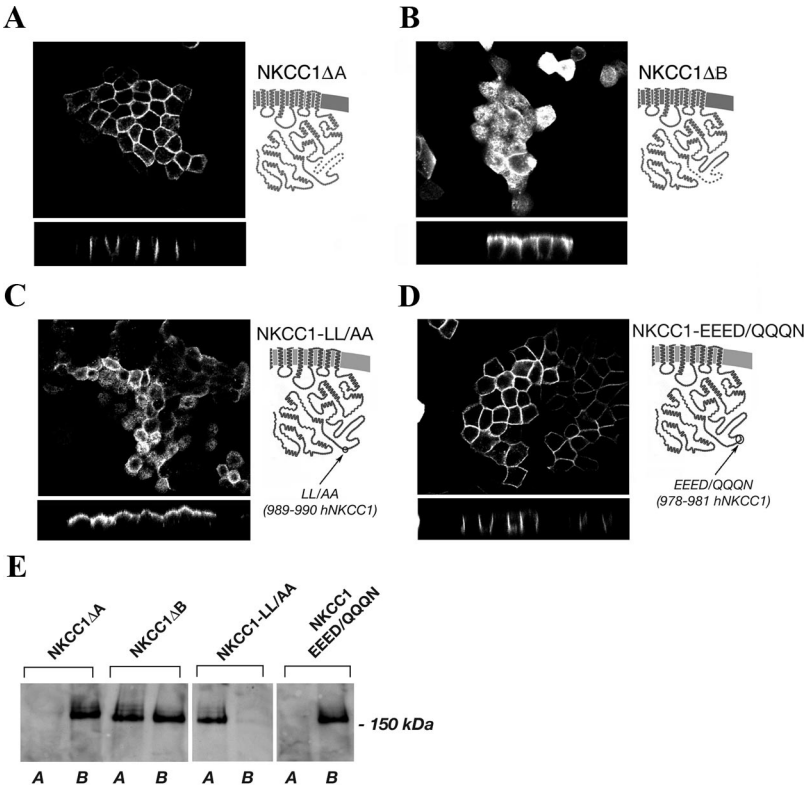

Figure 7. Localization of NKCC1ΔA, NKCC1ΔB, NKCC1-LL/AA, and NKCC1-EEED/QQQN mutants in stably transfected MDCK cells. (A and B) Deleted regions in NKCC1 are represented by dotted lines in the cartoons. Basolateral sorting information is contained in the ΔB region of NKCC1. (C) NKCC1-LL/AA mutant was localized on the apical membrane suggesting that this dileucine motif is the smallest component of the basolateral NKCC1 sorting signal. (D) NKCC1-EEED/QQQN mutant was localized on the basolateral membrane, suggesting that the EEED motif is not involved in the basolateral sorting. (E) Domain-selective cell surface biotinylation of NKCC1ΔA, NKCC1ΔB, NKCC1-LL/AA, and NKCC1-EEED/QQQN mutants.

A Dilucine Motif Is the Smallest Essential and Autonomous Component of the Basolateral Sorting Signal in the NKCC1 Protein

To determine whether the NKCC1 counterpart of the IV-V sequence is necessary for the NKCC1 basolateral localization, we made an NKCC1 deletion construct lacking these 77-amino acid residues. This protein was retained in an intracellular compartment (data not shown), perhaps as consequence of a conformational modification induced by the large deletion. In contrast, two smaller deletions encompassing the first and second half of the same region were tolerated, with results shown in Figure 7. Although removal of the first half of the IV-V sequence had no effect on the basolateral localization of NKCC1 (NKCC1ΔA; Figure 7A), removal of the second half resulted in a protein construct (NKCC1ΔB; Figure 7B), with an essentially randomized apical and basolateral distribution. These results strongly suggest that the second half of the IV-V sequence contains sorting information essential for basolateral delivery of NKCC1.

In a comparative analysis of the IV-V region sequence (Figure 9A) our attention was drawn to a dileucine sequence at residues 989–990 in hNKCC1, which is absent in NKCC2. Remarkably, mutagenesis of only these two residues to alanines resulted in essentially complete retargeting of the NKCC1 mutant (NKCC1-LL/AA) to the apical membrane, as shown in Figure 7C. That the mutation does not simply abolish basolateral sorting, but actually results in a strictly apical distribution strongly suggests that cryptic apical sorting information resides elsewhere in the NKCC1 molecule, and is masked by the effect of the strong basolateral dileucine motif.

Figure 7C clearly demonstrates that this dileucine motif constitutes the smallest essential component of the basolateral sorting signal in the NKCC1 protein. Other residues near the dileucine motif are also well conserved among NKCC1s in various species (Figure 9A), and we wondered whether these might be required in addition to the dileucine itself. Thus, we made mutations in a conserved acidic stretch (EEED mutated to QQQN) at −10 residues relative to the LL, in the conserved TQP at −3 (mutated to AAA), and in the conserved P at +8 (mutated to A). As illustrated in Figure 7D for EEED->QQQN (others not shown), none of these mutations had any effect on the distribution of NKCC1, as all of the mutants were found exclusively basolateral membrane. We also investigated a second dileucine 17 residues downstream: mutation of these leucines to alanines also did not alter the basolateral localization of NKCC1 (data not shown). Domain-selective cell surface biotinylation experiments confirmed the results obtained by immunolocalization analysis (Figure 7E). NKCC1ΔA was found among proteins selectively biotinylated at the basolateral surface, whereas NKCC1ΔB was available to biotin labeling from both the apical and basolateral sides. The LL/AA and EEED/QQQN mutants were exclusively labeled from the apical and the basolateral surfaces, respectively. Thus, it seems that the only critical residues in this basolateral sorting signal are the leucines identified at hNKCC 1 residues 989–990.

To determine whether the newly defined NKCC1 sorting region (IV-V region) is sufficient to function autonomously as a basolateral sorting determinant, we fused it to the terminus of PLAP-V. It can be clearly seen in Figure 8A that the IV-V region of NKCC1 is by itself sufficient to redirect the distribution of the PLAP-V construct from random localization at both membrane domains (Figure 4A, top) to exclusive localization at the basolateral membrane. As illustrated in Figure 8B, when we mutated the identified dileucine motif to dialanine in this construct, the basolateral sorting was disrupted just as it had been in NKCC1 itself, demonstrating again that the 989–990 dileucine is the critical motif in the NKCC1 sorting region. To verify whether the sorting region of NKCC1 is able to drive basolateral localization when it is expressed in the context of an apical chimera, we generated chimera III-IV+VI-term, which corresponds to the apical chimera III (Figure 2) containing the IV-V region of NKCC1. As shown in Figure 8C, chimera III-IV+VI-term was selectively expressed at the basolateral membrane. Thus, the IV-V sorting region of NKCC1 is able

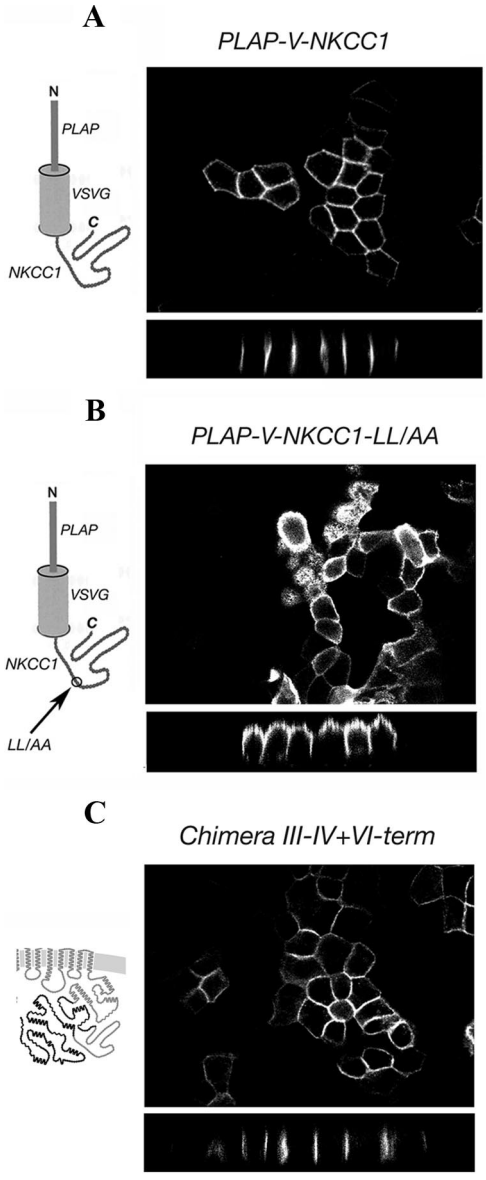

Figure 8. Cell surface localization of PLAP-V-NKCC1 constructs and chimera III-IV+VI-term. The structure of each construct is shown on the left of the panel in which its localization is depicted. (A) The IV-V region of NKCC1 carries autonomous basolateral sorting signals. (B) The dileucine is the critical motif in the NKCC1 IV-V sorting region. (C) The IV-V region of NKCC1 is sufficient to confer a fully basolateral localization to an apical chimera.

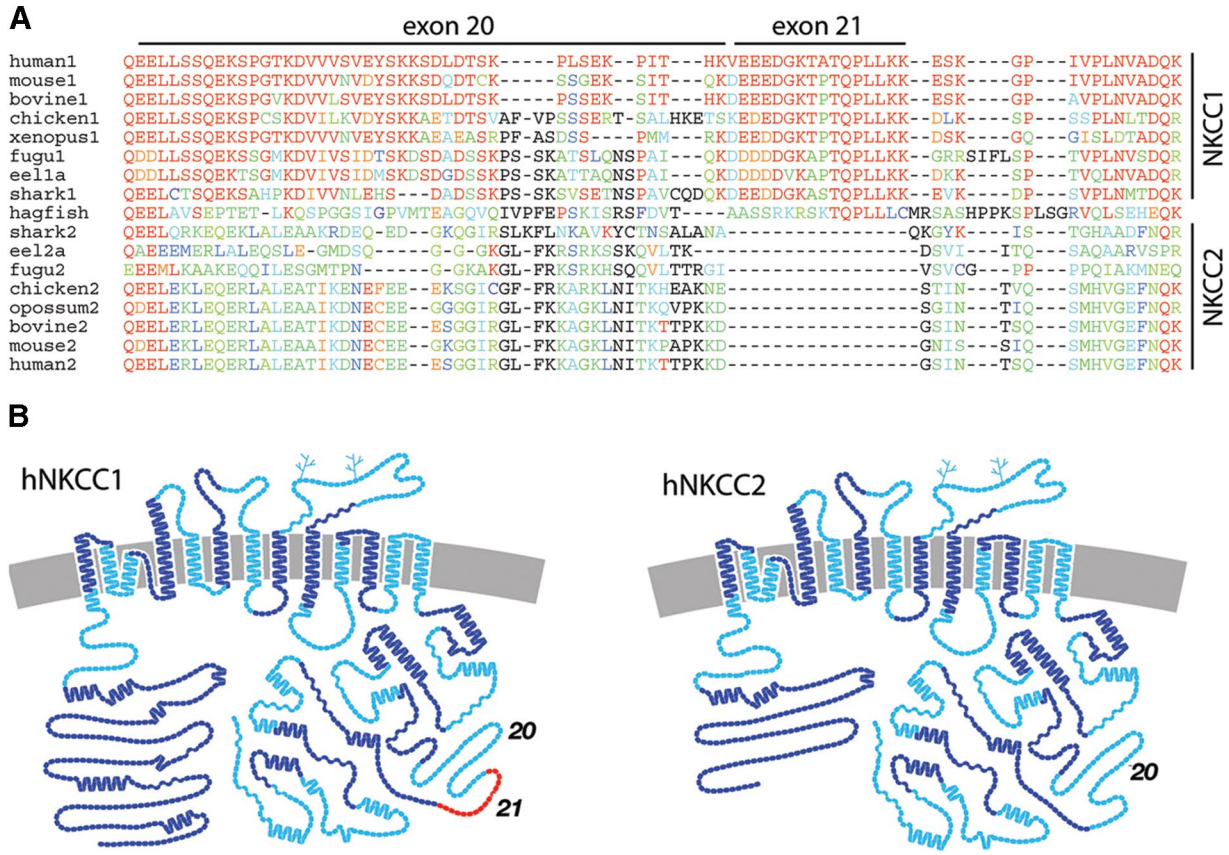

Figure 9. Exon structure of NKCCs. (A) Alignment of NKCC1 and NKCC2 sequences in the exon 20–21 region, color-coded by similarity to human NKCC1. (B) Exon organization of NKCC1 and NKCC2, with every other exon highlighted in light or dark blue. Exon 21, unique to NKCC1, is shown in red.

to function as an autonomous basolateral sorting signal in both an unrelated protein, and in intact NKCC.

A 16-Residue Exon Encoding the Basolateral Sorting Motif Is Present in NKCC1 and Absent from NKCC2

Comparison of the gene structures of NKCC1 and NKCC2 reveals that they have exactly the same set of exon boundaries, with one exception: as illustrated in Figure 9B, exon 21 of NKCC1 is absent from NKCC2. The sequence encoded by this exon is part of the NKCC1ΔB region, and it contains the NKCC1 dileucine sorting motif. The 16-residue sequence encoded by exon 21 is reasonably well conserved in vertebrate NKCC1s, with complete vertebrate conservation of the TQPLLKK sequence containing the dileucine (Figure 9A). NKCC1 and NKCC2 seem to have arisen from genome duplication early in vertebrate evolution: although in examining the closest prevertebrate sequences we have not found homology in this region with urchin or lancelet NKCCs (data not shown), we note the conservation of TQPLL in the single hagfish NKCC (Figure 9A). This indicates that the TQPLL sequence containing the dileucine motif was present in the ancestral NKCC and that subsequent to genome duplication exon 21 was lost from NKCC2, resulting in an apically targeted NKCC2 to complement a basolaterally targeted NKCC1.

DISCUSSION

In the present study, the structural basis for the polarized expression of the highly homologous Na-K-2Cl cotransporter isoforms NKCC1 and NKCC2 was elucidated. We demonstrated that the C termini contain sorting signals necessary for the basolateral localization of NKCC1 and the apical localization of NKCC2, respectively.

Analysis of the C termini by successive replacement of regions of the NKCC1 C terminus with the complementary sequences from the NKCC2 C terminus allowed us to narrow the region containing sorting information to an amino acid stretch located between the junction points of chimeras IV and V, corresponding to amino acids 930-1007 in NKCC1 and amino acids 807–884 in NKCC2.

The apical localization of the sequential chimeras demonstrated in Figure 2 could be due to the addition of an NKCC2-derived apical sorting signal to the NKCC1 backbone. It is also possible, however, that the removal of a primary basolateral sorting determinant from NKCC1 results in the apical localization of the resultant protein via a default mechanism. We consider the last possibility unlikely, however, because several exogenous proteins derived from different sources that lack sorting signals are delivered in a nonpolarized manner when expressed in MDCK cells (Gottlieb *et al*., 1986; Vogel *et al*., 1992). These observations thus strongly argue in favor of the presence of an active apical sorting signal in NKCC2. Moreover, the PLAP-V-NKCC2 protein, generated by the fusion of the region IV-V of NKCC2 with PLAP-V (Figure 4B), was delivered to the apical membrane, suggesting that this region of NKCC2 indeed carries autonomous apical sorting signals. This finding further supports the hypothesis that the polarized local-

ization of the apical chimeras is a product of an active sorting process rather than a default mechanism.

Unexpectedly, when this IV-V region of NKCC2 sequence was substituted into the context of NKCC1, the resulting chimera (chimera IV-V) was distributed randomly between the apical and basolateral domain, suggesting that this region of NKCC2 is not in itself sufficient to fully specify an apical localization when expressed in the context of NKCC1. However, we demonstrated that pairing of the NKCC2 IV-V region with the contiguous downstream region V-VI of NKCC2 is necessary and sufficient to induce a fully apical localization of the cotransporter. We propose that region V-VI of NKCC2 imposes a particular conformation upon the sequence determinant that constitutes the actual sorting signal in the region IV-V, allowing it to be recognized by the apical sorting machinery. This situation is reminiscent of that described for the apical sorting of the α-subunit of the gastric H,K-ATPase, where chimeras with the basolaterally sorted Na,K-ATPase have been used to identify three regions whose conformational interactions seem to affect sorting (Dunbar *et al*., 2000). Similarly, apical sorting signals have been identified in a short region of the N terminus of three apical members of the serpin family (Vogel *et al*., 2002). None of the individual amino acid residues making up this domain are required for the apical targeting that this amino acid stretch confers, suggesting that the apical secretion of the serpins by MDCK cells does not depend on a strictly conserved linear sequence but may instead depend on these proteins' conformations (Vogel *et al*., 2002). Grati *et al*. (2006) analyzed the molecular basis for the differential membrane trafficking of the plasma membrane calcium pumps PMCA1 and PMCA2 in hair cells of the inner ear. They found that the apical targeting of PMCA2 depends on the size but not on the sequence of a splice insert in its first intracellular loop, suggesting that the conformation of this cytoplasmic loop plays a role in apical sorting (Grati *et al*., 2006).

It has been suggested that detergent-resistant raft domains function as apical membrane targeting platforms. However, a correlation between apical targeting and association with detergent-resistant membranes was not observed when apical NKCC chimeras were analyzed, suggesting that the apical chimeras do not achieve their polarized distribution through any long-term, stable interactions with lipid rafts. The precise nature of the NKCC2 apical sorting determinants and the mechanism through which they are interpreted remain to be determined.

Newly synthesized proteins can reach the apical plasma membrane via either direct delivery from TGN or by transcytosis following delivery from the TGN to the basolateral membrane. For technical reasons, we were unable to verify whether the apical chimeras generated in this work were delivered to the apical membrane by a direct or indirect pathway. Thus, although in MDCK cells the majority of apical proteins have been shown to follow a direct route to the apical membrane, we cannot exclude the possibility that the NKCC apical chimeras may reach the apical surface through a pathway involving transcytosis.

In the basolateral NKCC1 the biochemical nature of the signal responsible for polarized sorting could be much more precisely determined. A comparative interspecies analysis of the amino acid region of NKCC1 carrying the presumptive basolateral sorting information revealed a highly conserved dileucine motif in position 989–990 in human NKCC1 that is absent in NKCC2. Mutagenesis of these two residues to alanine in NKCC1 resulted in the apical localization of the mutant protein (NKCC1-LL/AA), demonstrating that this dilucine motif constitutes the smallest essential component of the basolateral sorting signal in the NKCC1 protein.

The dileucine motif has been well characterized as a basolateral sorting signal in the cytoplasmic terminus of several membrane proteins that are delivered to the basolateral membrane. Dileucine motifs in the C terminus of the epithelial adhesion molecule E-cadherin (Miranda *et al*., 2001), sulfate/bicarbonate/oxalate anion exchange sat-1 (Regeer and Markovich, 2004), Fc receptors (Newton *et al*., 2005), and melanoma cell adhesion molecule (MCAM)-l cell adhesion molecule (Guezguez *et al*., 2006) direct each of these protein's basolateral sorting.

The surprising observation that the NKCC1-LL/AA mutant behaves as an exclusively apical protein suggests the presence of cryptic apical sorting information in this region of NKCC1 that specifically interacts with the apical sorting machinery once the dominant basolateral sorting signal is removed. The presence of multiple hierarchical targeting signals has been demonstrated for several transmembrane proteins, for which deletion of a basolateral targeting sequence reveals the existence of a subordinate apical targeting determinant (Yokode *et al*., 1992; Hobert and Carlin, 1995; Koivisto *et al*., 2001).

Analysis of the genomic structures of NKCC1 and NKCC2 shows that the two transporters have essentially identical intron–exon organization except that NKCC1 contains one additional exon. The additional exon 21 is only 16 amino acids in length and includes the dileucine sorting signal that we have identified in the C terminus of NKCC. The TQPLLKK sequence containing the dileucine is fully conserved in vertebrate NKCC1s, and the TQPLL sequence is also present in the single NKCC in hagfish (Hypotreti), the closest relative of true vertebrates. This observation indicates that the basolateral sorting motif was present in the ancestral genome, and that its loss from NKCC2 subsequent to genome duplication resulted in a vertebrate Na-K-Cl cotransporter that is apically targeted.

The MCAM is expressed as two isoforms, MCAM-l (long) and MCAM-s (short), differing by the cytoplasmic region generated by alternative splicing of exon 15 (Vainio *et al*., 1996). When expressed in MDCK cells, MCAM-l and MCAM-s are addressed to the basolateral and apical membranes, respectively. Exon 15 in MCAM-l includes a dileucine motif responsible for its basolateral localization. In contrast, a splice-induced frameshift produces apically-targeted MCAM-s, whose C terminus might interact with a postsynaptic density 95/disc-large/zona occludens domain (Guezguez *et al*., 2006). Our data demonstrate that, in addition to alternative splicing, loss of an exon at the genomic level after gene duplication can result in the creation two closely related gene products that manifest distinct sorting behaviors.

In NKCC1, exon 21 has been previously shown to be optionally spliced, so that although the encoded residues are present in NKCC1 in most tissues including secretory epithelia, they are absent from NKCC1 expressed in neuronal tissue (Randall *et al*., 1997). Consistent with our $^{86}Rb^{+}$ influx experiments reported in Figure 5, the absence of this sequence region has been shown to have no effect on NKCC1 function in transfected MDCK-LKC1 cells (Vibat *et al*., 2001). Dileucine motifs have been shown to function as dendritic targeting signals for a variety of proteins expressed in neurons, such as the Kv4.2 potassium channel (Rivera *et al*., 2003). NKCC1 functional activity has been demonstrated to be present on glutamatergic presynaptic nerve terminals projecting to ventromedial hypothalamic neurons and in the axon initial segment in cortical principal neurons, where it

creates an outwardly directed Cl^--driving force associated with GABA-induced presynaptic depolarization (Jang *et al*., 2001; Khirug *et al*., 2008). The axonal expression of neuronal NKCC1 activity is entirely consistent with the idea that loss of the dendritic targeting information inherent in the exon 21 dileucine motif, in this case by alternative splicing, provides individual cell types with the capacity to direct NKCC activity to the specific plasma membrane domains demanded by each cell's physiological requirements. It will be interesting to determine, therefore, whether the neuronal splice isoform of NKCC1 is, in fact, completely restricted in its distribution to axonal membranes.

Our data indicated that the IV-V region of the C terminus of NKCC2 is required for apical sorting of the cotransporter protein. The sequence of the IV-V region of NKCC1 corresponds roughly to the residues encoded by NKCC1 exons 20 and 21 (Figure 9B). It is important to note that all of the exon–intron boundaries surrounding exons 20–22 are symmetrical (that is, all are phase 1 with regard to the reading frame), which means that exons can theoretically be used or not without affecting the reading frame of the rest of the C terminus. The sequence of exon 20 is extremely poorly conserved between NKCC1 and NKCC2 (Figure 9A), further suggesting the interesting possibility that the apical sorting of NKCC2 is a product both of the loss of the dileucine motif encoded by exon 21 as well as the unique degree of divergence in the sequence of NKCC2 exon 20 from that of its counterpart in NKCC1.

Among the 16 dileucines in the NKCC1 sequence, the dileucine in exon 21 is identified here as containing functionally significant basolateral targeting information. On the basis of primary sequence, the secondary structure of the IV-V region of NKCCs is predicted to be relatively disordered (Supplemental Figure 2). We have found that neither the upstream acidic region nor the conserved TQP preceding the dileucine are needed for basolateral sorting of NKCC1. Thus, it is possible that surface exposure and peptide flexibility are two elements that enable this particular dileucine to direct basolateral targeting. Future structural studies will be required to understand both why the exon 21 dileucine motif is uniquely accessible to the sorting machinery, and how the IV-V and V-VI regions of the NKCC2 sequence collaborate to create a conformation that specifies apical targeting.

ACKNOWLEDGMENTS

We thank Esther Bashi and Vanathy Rajendran for experimental assistance and Paul Isenring and Deborah Lynn for early steps in making chimera 1–2-1. This research was supported by National Institute Health Grant DK-17433 (BFIII, MJC).

REFERENCES

Brindikova, T. A., Bourcier, N., Torres, B., Pchejetski, D., Gekle, M., Maximov, G. V., Montminy, V., Insel, P. A., Orlov, S. N., and Isenring, P. (2003). Purinergic-induced signaling in C11-MDCK cells inhibits the secretory Na-K-Cl cotransporter. Am. J. Physiol. Cell. Physiol. *285*, C1445–C1453.

Brown, A., Muth, T., and Caplan, M. (2004). The COOH-terminal tail of the GAT-2 GABA transporter contains a novel motif that plays a role in basolateral targeting. Am. J. Physiol. Cell. Physiol. *286*, C1071–C1077.

Chuang, J. Z., and Sung, C. H. (1998). The cytoplasmic tail of rhodopsin acts as a novel apical sorting signal in polarized MDCK cells. J. Cell. Biol. *142*, 1245–1256.

Del Castillo, I. C., Fedor-Chaiken, M., Song, J. C., Starlinger, V., Yoo, J., Matlin, K. S., and Matthews, J. B. (2005). Dynamic regulation of Na(+)-K(+)-2Cl(−) cotransporter surface expression by PKC-{epsilon} in Cl(−)-secretory epithelia. Am. J. Physiol. Cell. Physiol. *289*, C1332–C1342.

Delpire, E., Rauchman, M. I., Beier, D. R., Hebert, S. C., and Gullans, S. R. (1994). Molecular cloning and chromosome localization of a putative basolateral Na(+)-K(+)-2Cl− cotransporter from mouse inner medullary collecting duct (mIMCD-3) cells. J. Biol. Chem. *269*, 25677–25683.

Delpire, E. (2000). Cation-chloride cotransporters in neuronal communication. News Physiol. Sci. *15*, 309–312.

Dunbar, L. A., Aronson, P., and Caplan, M. J. (2000). A transmembrane segment determines the steady-state localization of an ion-transporting adenosine triphosphatase. J. Cell. Biol. *148*, 769–778.

Gimenez, I., and Forbush, B. (2003). Short-term stimulation of the renal Na-K-Cl cotransporter (NKCC2) by vasopressin involves phosphorylation and membrane translocation of the protein. J. Biol. Chem. *278*, 26946–26951.

Glorioso, N., Filigheddu, F., Troffa, C., Soro, A., Parpaglia, P. P., Tsikoudakis, A., Myers, R. H., Herrera, V. L., and Ruiz-Opazo, N. (2001). Interaction of alpha(1)-Na,K-ATPase and Na,K,2Cl-cotransporter genes in human essential hypertension. Hypertension *38*, 204–209.

Gottlieb, T. A., Beaudry, G., Rizzolo, L., Colman, A., Rindler, M., Adesnik, M., and Sabatini, D. D. (1986). Secretion of endogenous and exogenous proteins from polarized MDCK cell monolayers. Proc. Natl. Acad. Sci. USA *83*, 2100–2104.

Grati, M., Aggarwal, N., Strehler, E. E., and Wenthold, R. J. (2006). Molecular determinants for differential membrane trafficking of PMCA1 and PMCA2 in mammalian hair cells. J. Cell. Sci. *119*, 2995–3007.

Guezguez, B., Vigneron, P., Alais, S., Jaffredo, T., Gavard, J., Mege, R. M., and Dunon, D. (2006). A dileucine motif targets MCAM-l cell adhesion molecule to the basolateral membrane in MDCK cells. FEBS Lett. *580*, 3649–3656.

Haas, M., and Forbush, B., 3rd. (2000) The Na-K-Cl cotransporter of secretory epithelia. Annu. Rev. Physiol. *62*, 515–534.

Hobert, M., and Carlin, C. (1995). Cytoplasmic juxtamembrane domain of the human EGF receptor is required for basolateral localization in MDCK cells. J. Cell. Physiol. *162*, 434–446.

Igarashi, P., Vanden Heuvel, G. B., Payne, J. A. and Forbush, B., 3rd. (1995) Cloning, embryonic expression, and alternative splicing of a murine kidney-specific Na-K-Cl cotransporter. Am. J. Physiol. *269*, F405–F418.

Inukai, K., Shewan, A. M., Pascoe, W. S., Katayama, S., James, D. E., and Oka, Y. (2004). Carboxy terminus of glucose transporter 3 contains an apical membrane targeting domain. Mol. Endocrinol. *18*, 339–349.

Isenring, P., Jacoby, S. C. and Forbush, B., 3rd. (1998a). The role of transmembrane domain 2 in cation transport by the Na-K-Cl cotransporter. Proc. Natl. Acad. Sci. USA *95*, 7179–7184.

Isenring, P., Jacoby, S. C., Payne, J. A. and Forbush, B., 3rd. (1998b). Comparison of Na-K-Cl cotransporters. NKCC1, NKCC2, and the HEK cell Na-L-Cl cotransporter. J. Biol. Chem. *273*, 11295–11301.

Jang, I. S., Jeong, H. J., and Akaike, N. (2001). Contribution of the Na-K-Cl cotransporter on GABA(A) receptor-mediated presynaptic depolarization in excitatory nerve terminals. J. Neurosci. *21*, 5962–5972.

Ji, W., Foo, J. N., O'Roak, B. J., Zhao, H., Larson, M. G., Simon, D. B., Newton-Cheh, C., State, M. W., Levy, D., and Lifton, R. P. (2008) Rare independent mutations in renal salt handling genes contribute to blood pressure variation. Nat. Genet. *40*, 592–599.

Karim-Jimenez, Z., Hernando, N., Biber, J., and Murer, H. (2001). Molecular determinants for apical expression of the renal type IIa Na+/Pi-cotransporter. Pflugers Arch. *442*, 782–790.

Koivisto, U. M., Hubbard, A. L., and Mellman, I. (2001). A novel cellular phenotype for familial hypercholesterolemia due to a defect in polarized targeting of LDL receptor. Cell *105*, 575–585.

Khirug, S., Yamada, J., Afzalov, R., Voipio, J., Khiroug, L., and Kaila, K. (2008). GABAergic depolarization of the axon initial segment in cortical principal neurons is caused by the Na-K-2Cl cotransporter NKCC1. J. Neurosci. *28*, 4635–4639.

Miranda, K. C., Khromykh, T., Christy, P., Le, T. L., Gottardi, C. J., Yap, A. S., Stow, J. L., and Teasdale, R. D. (2001). A dileucine motif targets E-cadherin to the basolateral cell surface in Madin-Darby canine kidney and LLC-PK1 epithelial cells. J. Biol. Chem. *276*, 22565–22572.

Muth, T. R., and Caplan, M. J. (2003). Transport protein trafficking in polarized cells. Annu. Rev. Cell. Dev. Biol. *19*, 333–366.

Newton, E. E., Wu, Z., and Simister, N. E. (2005). Characterization of basolateral-targeting signals in the neonatal Fc receptor. J. Cell. Sci. *118*, 2461–2469.

Obermuller, N., Kunchaparty, S., Ellison, D. H., and Bachmann, S. (1996). Expression of the Na-K-2Cl cotransporter by macula densa and thick ascending limb cells of rat and rabbit nephron. J. Clin. Invest. *98*, 635–640.

Ortiz, P. A. (2006). cAMP increases surface expression of NKCC2 in rat thick ascending limbs: role of VAMP. Am. J. Physiol. Renal Physiol. *290*, F608–F616.

Paredes, A., Plata, C., Rivera, M., Moreno, E., Vazquez, N., Munoz-Clares, R., Hebert, S. C., and Gamba, G. (2006). Activity of the renal Na+-K+-2Cl− cotransporter is reduced by mutagenesis of N-glycosylation sites: role for protein surface charge in Cl− transport. Am. J. Physiol. Renal Physiol. *290*, F1094–F1102.

Payne, J. A. and Forbush, B., 3rd. (1994). Alternatively spliced isoforms of the putative renal Na-K-Cl cotransporter are differentially distributed within the rabbit kidney. Proc. Natl. Acad. Sci. USA *91*, 4544–4548.

Pedersen, M., Carmosino, M., and Forbush, B. (2008). Intramolecular and intermolecular fluorescence resonance energy transfer in fluorescent protein-tagged Na-K-Cl cotransporter (NKCC1): sensitivity to regulatory conformational change and cell volume. J. Biol. Chem. *283*, 2663–2674.

Randall, J., Thorne, T., and Delpire, E. (1997). Partial cloning and characterization of Slc12a 2, the gene encoding the secretory Na+-K+-2Cl− cotransporter. Am. J. Physiol. *273*, C1267–C1277.

Regeer, R. R., and Markovich, D. (2004). A dileucine motif targets the sulfate anion transporter sat-1 to the basolateral membrane in renal cell lines. Am. J. Physiol. Cell. Physiol. *287*, C365–C372.

Rivera, J. F., Ahmad, S., Quick, M. W., Liman, E. R., and Arnold, D. B. (2003). An evolutionarily conserved dileucine motif in Shal K+ channels mediates dendritic targeting. Nat. Neurosci. *6*, 243–250.

Rodriguez-Boulan, E., Kreitzer, G., and Musch, A. (2005). Organization of vesicular trafficking in epithelia. Nat. Rev. Mol. Cell. Biol. *6*, 233–247.

Roush, D. L., Gottardi, C. J., Naim, H. Y., Roth, M. G., and Caplan, M. J. (1998). Tyrosine-based membrane protein sorting signals are differentially interpreted by polarized Madin-Darby canine kidney and LLC-PK1 epithelial cells. J. Biol. Chem. *273*, 26862–26869.

Simon, D. B., Karet, F. E., Hamdan, J. M., DiPietro, A., Sanjad, S. A., and Lifton, R. P. (1996). Bartter's syndrome, hypokalaemic alkalosis with hypercalciuria, is caused by mutations in the Na-K-2Cl cotransporter NKCC2. Nat. Genet. *13*, 183–188.

Vainio, O., Dunon, D., Aissi, F., Dangy, J. P., McNagny, K. M., and Imhof, B. A. (1996). HEMCAM, an adhesion molecule expressed by c-kit+ hemopoietic progenitors. J. Cell. Biol. *135*, 1655–1668.

Vibat, C. R., Holland, M. J., Kang, J. J., Putney, L. K., and O'Donnell, M. E. (2001). Quantitation of Na+-K+-2Cl− cotransport splice variants in human tissues using kinetic polymerase chain reaction. Anal. Biochem. *298*, 218–230.

Vogel, L. K., Spiess, M., Sjostrom, H., and Noren, O. (1992). Evidence for an apical sorting signal on the ectodomain of human aminopeptidase N. J. Biol. Chem. *267*, 2794–2797.

Vogel, L. K., Sahkri, S., Sjostrom, H., Noren, O., and Spiess, M. (2002). Secretion of antithrombin is converted from nonpolarized to apical by exchanging its amino terminus for that of apically secreted family members. J. Biol. Chem. *277*, 13883–13888.

Yokode, M., Pathak, R. K., Hammer, R. E., Brown, M. S., Goldstein, J. L., and Anderson, R. G. (1992). Cytoplasmic sequence required for basolateral targeting of LDL receptor in livers of transgenic mice. J. Cell. Biol. *117*, 39–46.